

Influence of Surface Scattering on the Radio-Frequency Size Effect*

G. E. Juras

Department of Physics, Case Western Reserve University, Cleveland, Ohio 44106

(Received 5 March 1970)

The surface impedance of a thin metal plate excited by a rf electromagnetic field is calculated as a function of external dc magnetic field applied in the plane of the plate under the nonlocal conditions of the anomalous skin effect. A linearized Boltzmann equation in the relaxation time approximation for isotropic bulk scattering is solved by means of a generalized kinetic formulation which (i) describes the surface scattering by means of a *specularity function* that can depend on the angle of collision of the electron trajectories with the surface, and which (ii) contains an *ineffectiveness parameter* in the nonlocal form of Ohm's law, thus providing a measure for the possibility that electrons colliding with the boundaries are less effective than bulk electrons in linking the current density at one point of the conductor with the electric field at another point. This generalized path-integral solution of the Boltzmann equation is coupled with Maxwell's equations, and the resulting integrodifferential equation is solved for the spatial distribution of the electric field inside the metal plate using the numerical procedure discussed in an earlier publication by the author. This is done for both the symmetric and antisymmetric modes of excitation of the plate by the rf field in the case of a model cylindrical Fermi surface. The resulting curves for the surface impedance versus the applied dc magnetic field exhibit characteristic features which are greatly influenced by the explicit choice of the specularity function and/or the ineffectiveness parameter. It is suggested that these features can be used in conjunction with experiment to determine the correct parameters for the surface scattering mechanism.

I. INTRODUCTION

The surface impedance of a thin metal plate excited by an electromagnetic field of frequency ω under the nonlocal conditions of the anomalous skin effect exhibits resonant structure as a function of an external dc magnetic field \vec{H} .¹ Of the many resonances that occur as a result of the matching between either the temporal or the spatial characteristics of the rf field with those of the orbital motion of the electrons, we will limit ourselves to the discussion of the surface impedance variations observed in the simple geometry of Fig. 1. Here, rf current layers $\vec{j}(z) = j(z)e^{-i\omega t}\hat{y}$ of effective skin depth δ are set up by means of coils on both sides of a plate of thickness d (either symmetrically or antisymmetrically) in anomalous skin effect conditions. This is precisely the configuration used in the study of the radio-frequency size effect (RFSE).¹ The coordinate z measures the depth inside the plate from the $z=0$ surface. The external dc magnetic field is applied in the plane of the plate and in the transverse direction with respect to the rf current, $\vec{H} = H\hat{x}$.

As we do not plan to examine dispersion effects in this paper, we will assume a cylindrical Fermi surface for the electrons in the plate. This means that all electrons describe circular trajectories perpendicular to \vec{H} (see Fig. 1) with the common frequency $\Omega = |e|H/mc$, where $-|e|$ and m are the

charge and mass of a free electron. Here we note that we use the term "trajectory" to describe motion in real space (as opposed to the term "orbit" for motion in momentum space) and that we distinguish between "surface" and "bulk" trajectories depending upon whether a trajectory collides or does not collide with either surface (see Fig. 1). In the cylindrical Fermi-surface model the velocity of every electron has no component along the magnetic field and, for electrons on the Fermi surface, this velocity is simply given by

$$\vec{v} \equiv v_F \vec{\mu} = v_F (\hat{y} \cos \phi + \hat{z} \sin \phi), \quad (1.1)$$

where v_F is the Fermi velocity and ϕ is the dimensionless "orbit" or "phase" variable² (with $\dot{\phi} = \Omega$) which is used in place of the real time t and which characterizes the direction of \vec{v} as the electron moves on its circular trajectory. The height of the Fermi cylinder, Δp_x , is adjusted in terms of the correct density of electrons, n , for a free electron metal of Fermi momentum $p_F = \hbar k_F$, $n = 2\pi p_F^2 \Delta p_x / (2\pi\hbar)^3$.

The size of the electronic trajectories is inversely proportional to the magnetic field. For a critical magnetic strength equal to

$$H_d = \frac{2(\hbar c / e) k_F}{d},$$

these trajectories will span completely a plate of thickness d . This means that for values of H less than H_d all of the electrons that pass through any point z of the plate at a time t collided with either

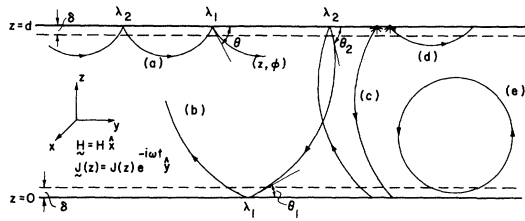


FIG. 1. Free-electron trajectories spanning a thin metal plate of thickness d in the presence of an external dc magnetic field $\vec{H} = H\hat{x}$. (a) and (b) are specularly reflected surface trajectories, (c) and (d) are diffusely scattered surface trajectories, and (e) is an effective bulk trajectory.

surface at some earlier time – they all describe surface trajectories. For values of H greater than H_d some of the electrons passing through some points z of the plate never collided with either surface, i.e., they describe bulk trajectories. For H between H_d and $H_d + \Delta H$, where $\Delta H \approx 2\delta/d$ in particular, electrons moving nearly parallel to the faces of the plate (with $v_z \approx 0$), when passing through the skin layer defined by $z=0$ and $z=\delta$, will pass through the layer defined by $z=d$ and $z=d-\delta$ at the second surface, again with $v_z \approx 0$ and without colliding with that surface. Such bulk electrons are said to be *effective* in that they spend a lot of their mean free time in the skin layers and they can absorb energy from the rf field more effectively than surface electrons.

The primary line of the RFSE¹ is the signature of the change in the resonant response of the plate (specified by its surface impedance) to the driving rf field as the external dc magnetic field is varied from values of H just below to values just above H_d . The left-most sharp variation in the RFSE line shape is dictated by the first length of the problem, the thickness of the plate d , and it coincides with the critical field H_d which signals the complete disappearance of the surface trajectories of the type (c) and the appearance of bulk trajectories of the type (e) in Fig. 1. The width of this line, $\Delta H/H_d$, is defined by the second length of the problem, the effective skin depth δ , and is approximately given by $2(\delta/d)$. The detailed shape of the line between H_d and $H_d + \Delta H$ reflects the spatial inhomogeneity of the rf field in the skin layers, for it is this part of the field with which the effective electrons interact most effectively in this region of magnetic field values. The symmetry of the line depends on the mode of excitation, the signal for the symmetric mode being the reverse of that for the antisymmetric mode. This means that the line registers the constructive (or destructive) interference between the driving currents in the one

skin layer and the currents from the second skin layer which are transmitted by the effective electron trajectories with diameters ranging from d to $(d - 2\delta)$. Since this interference is important for the existence of the effect, it becomes necessary to have specimens with mean free paths about as large as the thickness of the plate in order to observe a signal with significant amplitude. The third length of the problem, then, the mean free path, affects the amplitude of the RFSE line.

With regard to the only temporal parameters of the coupling, the two frequencies ω and Ω , we note that for most RFSE experiments $\omega \ll \Omega$, so that the electrons see a nearly static field each time they go through the skin layers. The RFSE resonance is a spatial resonance. There is no matching of frequencies as there is in the temporal Azbel-Kaner cyclotron resonance. The radio frequency ω simply establishes the effective skin depth δ which makes the RFSE line sharp.

So far in the discussion, the two faces of the plate which are normal to the z direction have been tacitly understood to be two perfect planes that simply restrict the excursions of the electrons within the plate. This is enough to dictate the position of the RFSE primary line. It is true that the surface represents a large (several electron volts) and abrupt potential barrier which is virtually impenetrable to the electrons; upon collision with the surface, the electrons are reflected back into the metal. However, the two following basic questions need to be asked: (1) How are the electrons reflected at the surface? (2) How does the specific surface scattering mechanism affect the structure of the surface impedance versus applied magnetic field?

In the absence of a microscopic theory of surface scattering, an answer has been given to the first question in terms of a phenomenological model, first proposed by Fuchs,³ in which a single specularly parameter p is supposed to describe the surface scattering mechanism. In the Fuchs model, p is the probability that an electron will be specularly scattered (the z component of its velocity changing sign upon reflection) while $1-p$ is the probability that the electron will be diffusely scattered at the surface. Diffuse scattering means that for any given angle of incidence the angle of reflection is random, so that the drift velocity of the electron after collision with the surface is zero on the average and the subsequent contribution of that electron to the conductivity vanishes. In Fig. 1, trajectories (a) and (b) are specularly scattered while trajectories (c) and (d) are diffusely scattered at the surface.

In a recent letter,⁴ the single specularly parameter of Fuchs has been generalized into a *specular-*

ity function $S(\theta)$ which, in general, will depend on θ , the angle of collision of a surface trajectory with the surface (see Fig. 1). The dependence on θ will provide a phenomenological description of the possibility that electrons with small angles of collision will be specularly scattered while electrons with large angles of collision will be diffusely scattered.

Inasmuch as the explicit nature of the RFSE line (mostly its amplitude) depends very critically on the effectiveness of the electrons to carry currents from one part of the conductor to another, under the nonlocal conditions of the anomalous skin effect, we introduce in this paper an additional parameter, which we call the *ineffectiveness parameter* and which is supposed to provide a measure of how much less effective (in carrying information from one point of the conductor to another) are the surface electrons as compared with the bulk electrons. This ineffectiveness parameter η amounts to describing the surface electrons with a surface mean free path l_s such that

$$l_s = \eta \cdot l, \quad 0 \leq \eta \leq 1,$$

where l is the mean free path for bulk electrons. In this connection, we note that one might simulate surface roughness by assuming a z -dependent mean free path, as was assumed in Ref. 5 for another related surface impedance calculation.

In Sec. II of this paper we extend the kinetic formalism already discussed by the author^{4,6} to include both the specularly function and the ineffectiveness factor, and in Sec. III we carry out model calculations so as to bring out the explicit influence of the different choices of the surface scattering parameters on the line shape of the RFSE.

II. FORMAL BACKGROUND

Maxwell's equations for the problem discussed in the Sec. I reduce to

$$\frac{\partial^2 E}{\partial z^2} = -i \frac{4\pi\omega}{c^2} j(z), \quad (2.1)$$

in the system of coordinates shown in Fig. 1, where $E(z)$ is the y component of the rf electric field inside the plate. The current density in (2.1) for a model cylindrical Fermi surface [see Eq. (1.1)] is

$$j(z) = (\sigma_0 / \pi \Omega \tau) \int_0^{2\pi} d\phi \mu_y(\phi) I(\phi, -\infty) \quad (2.2a)$$

in Chambers's⁷ kinetic formulation; here

$$I(\phi, -\infty) = \int_{-\infty}^{\phi} d\phi' \exp[-\gamma(\phi - \phi')] \mu_y(\phi') \times E[z - \Omega^{-1} \int_{\phi'}^{\phi} d\phi'' v_z(\phi'')] \quad (2.2b)$$

and

$$\gamma = (1 - i\omega\tau) / \Omega\tau, \quad (2.2c)$$

the collisions of electrons with an imperfect infinite lattice being described phenomenologically by a mean free path $l = v_F \tau$, in which case the static conductivity is equal to $\sigma_0 = ne^2 \tau / m$.

For a specimen of finite thickness, the integral of (2.2b) over the history of an electron which at "time" ϕ is at the point z of the conductor has been generalized⁴ to

$$I(\phi, -\infty) = I(\phi, \lambda_1) + \sum_{n=2}^{\infty} \left(\prod_{i=1}^{n-1} S(\theta_i) \right) \times \exp[-\gamma(\lambda_{i-1} - \lambda_i)] I(\lambda_{n-1}, \lambda_n), \quad (2.3a)$$

where

$$I(\lambda_{n-1}, \lambda_n) = \int_{\lambda_n}^{\lambda_{n-1}} d\phi' \exp[-\gamma(\lambda_{n-1} - \phi')] \times \mu_y(\phi') E[\xi_n(\phi')] \quad (2.3b)$$

and

$$\xi_n(\phi') = \xi_{n-1}(\lambda_{n-1}) - \Omega^{-1} \int_{\phi'}^{\lambda_{n-1}} d\phi'' v_z(\phi''),$$

$$\text{with } \xi_0(\lambda_0) \equiv \xi_0(\phi) = z. \quad (2.3c)$$

This generalization was carried out in order to allow for the possibility that surface electrons which collided with the $z=0$ (or the $z=d$) surface at the "instants" λ_n (previous to ϕ), defined by

$$\xi_n(\lambda_n) = 0 \text{ (or } d), \quad \phi \geq \lambda_{n-1} \geq \lambda_n, \quad (2.3d)$$

will continue on a specularly reflected path with a probability reduced by the factor

$$S(\theta_n), \quad 0 \leq S(\theta_n) \leq 1$$

after the n th collision (with an angle of collision equal to θ_n). For bulk electrons the integral of (2.2b) remains unmodified.

Equation (2.2) or its generalization (2.3) is the nonlocal form of Ohm's law which relates through an integral conductivity operator the electric field at the point

$$z' = z - \Omega^{-1} \int_{\phi}^{\phi} d\phi'' v_z(\phi'')$$

of the plate with the current density at z . A bulk electron which received from the electric field at z' an energy increment equal to

$$(|e| d\phi' / \Omega) \vec{v}(\phi') \cdot \vec{E}(z')$$

during the time interval from ϕ' to $\phi' + d\phi'$ carries the impact of that encounter to the point z at a later time ϕ with an exponentially decreasing probability $\exp[-\gamma(\phi - \phi')]$, (2.4)

where the bulk "time" constant γ is given by (2.2c).

It is through this exponential that we introduce the ineffectiveness parameter η , mentioned in Sec. I. For surface electrons the exponential of (2.4) trivially becomes

$$\exp[-\gamma_s(\phi - \phi')], \quad (2.5)$$

where the surface "time" constant $\gamma_s = \gamma/\eta$, $0 \leq \eta \leq 1$, replaces the bulk constant γ . The "memory" of surface electrons, as charge carriers which collide with the surfaces in addition to colliding with the vibrating lattice, decays exponentially over a distance l_s shorter than the bulk mean free path l by the ineffectiveness factor η , $l_s = \eta l$.

Completely diffuse and completely specular surface scattering can easily be expressed in terms of the extreme values of η , $\eta = 0$ and $\eta = 1$. As we integrate backwards in time from ϕ to $-\infty$ in (2.3a), the diffuse assumption means $\eta = 1$ for $\phi \geq \phi' \geq \lambda_1$, where λ_1 is the instant of the last collision (before ϕ) with either surface (see Fig. 1), and $\eta = 0$ for $\lambda_1 \geq \phi' \geq -\infty$; only the first term in (2.3a) survives. The electron upon collision with the surface "sticks" to it, a rather unphysical destiny from a conservation-of-probability point of view. On the other hand, the specular assumption means $\eta = 1$ for all times earlier than ϕ . In this case, collisions with the surface, even though they deflect the electrons through angles that can be as large as 180° , are supposed not to change the mean free path of the surface electrons to anything other than the bulk value. Clearly, an ineffectiveness parameter of intermediate value might be the more realistic assumption to make.

Substituting (2.2) into (2.1), after properly incorporating the specular function $S(\theta)$ through (2.3) and the ineffectiveness parameter η through (2.5), yields an integrodifferential equation which we solve for the unknown $E(z)$, subject to the boundary conditions $E(0) = \pm E(d) = 1$, by making use of the numerical model described in Ref. 6. The boundary condition $E(0) = -E(d)$ corresponds to the bilateral antisymmetric (BA) mode of excitation of the plate by the rf field. The bilateral symmetric (BS) mode corresponds to $E(0) = +E(d)$.

From the function $E(z)$, calculated for every value of the external dc magnetic field H , we obtain the surface impedance

$$Z(H) = \frac{i(4\pi\omega/c^2)E(z)}{E'(z)} \Big|_{z=0+} = \frac{4\pi\omega}{c^2} (R + iX) \quad (2.6)$$

as a function of H . It is the surface resistance R (or $\partial R/\partial H$), related to the fraction of incident power absorbed by the sample, and the surface reactance X (or $\partial X/\partial H$), related to inductance changes in the exciting coil, which are measured experimentally in order to register the response of the metal plate

to the external fields.

III. RESULTS AND DISCUSSION

We now present the calculated surface resistance $R(H)$ and surface reactance $X(H)$ curves for different choices of the surface and bulk scattering parameters. These parameters are the specular function $S(\theta)$, the ineffectiveness factor $\eta = l_s/l$, and the bulk mean free path l (or rather the ratio l/d which we denote by κ). In all of the subsequent calculations the rf $\omega/2\pi$ has been taken to be equal to 1 MHz, i.e., it is such that $\delta \ll d$ and $\omega \ll \Omega$, where Ω is the cyclotron frequency and δ is an effective skin depth.

The line shapes for the case of completely specular surface scattering [$S(\theta) \equiv p = 1$ for all θ , $\eta = 1$, $\kappa = 1$] are shown in Fig. 2 together with the corresponding line shapes for the case of completely diffuse surface scattering [$S(\theta) \equiv p = 0$ for all θ , $\eta = 1$, $\kappa = 1$] in order to facilitate comparison of the two sets of curves. The following observations are to be made:

(a) The surface resistance R (diffuse, BA) varies smoothly with H (it is flat) for $H < H_d$, while R (specular, BA) extrapolates to a peak at $H = 0$. Experimentally a peak in R is in fact observed.⁸

(b) The ratio Z (diffuse)/ Z (specular) at $H = 0$ is approximately equal to $\frac{9}{8}$ in agreement with the early results of Reuter and Sondheimer⁹ for a semi-infinite free-electron metal. In addition, $X(0) \approx -\sqrt{3} R(0)$ for both surface scattering assumptions, also agreeing approximately with the results of Ref. 9.

(c) The shape of the R (diffuse, BA) line beginning at $H/H_d = 1$ exhibits a definite dip immediately after $H/H_d = 1$ before a subsequent large peak. The initial dip is missing in the R (specular, BA) line shape, while the subsequent peak remains, although with a smaller amplitude. The initial dip in the surface resistance is present in the diffuse case because the appearance at $H/H_d = 1$ of the effective bulk trajectories of the type shown in Fig. 1 signals a situation of substantially more surface conductivity than the conductivity due to the surface trajectories of the type c shown in Fig. 1 present at $H/H_d < 1$. On the other hand, the appearance of the effective bulk trajectories at $H/H_d = 1$ for the specular case is not enough to produce a dip in R because of the destructive interference between the effective bulk trajectories and the ever present effective skipping surface trajectories (of the type as shown in Fig. 1) which by scalloping inside the skin layers produce surface currents in the opposite direction than those carried by the bulk trajectories. It is the presence of these conducting skipping surface trajectories in the specular case and their absence in the diffuse case that also makes the am-

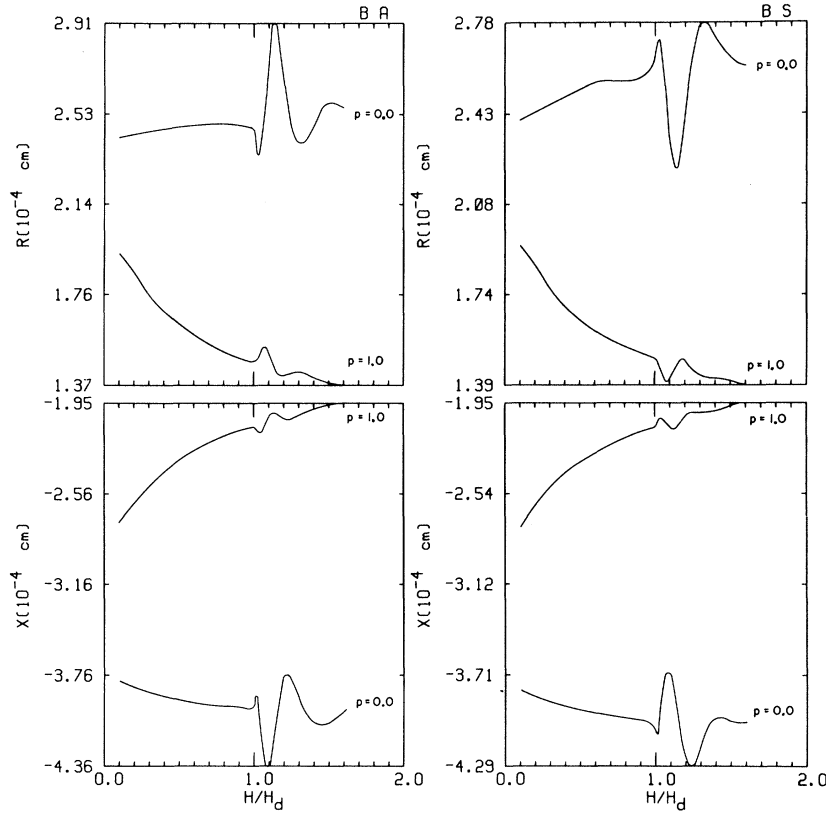


FIG. 2. Surface resistance R and the surface reactance X as functions of the external dc magnetic field (in units of H_d , the resonant field at which the thickness of the plate is equal to the diameter of the trajectories) for both modes of excitation of the plate by the rf field [bilateral antisymmetric (BA) and bilateral symmetric (BS)] and for both extreme surface scattering assumptions [diffuse ($p=0$) and specular ($p=1$)].

plitude of the peak in R (specular, BA) smaller than that of R (diffuse, BA).

(d) The line shape for $\partial R/\partial H$ (BA) in potassium as measured by Koch and Wagner¹⁰ does not show the initial dip present in the calculated line shape of R (diffuse, BA); it is the specular line shape that agrees with the above experiment. This is consistent with the fact that it was in the same laboratory that good surface preparation allowed the discovery of magnetic surface states,¹¹ whose very existence depends on the assumption of specular scattering.

On the other hand, the line shape reported by Walsh *et al.*,¹² also in potassium, does not agree with either of the above extreme assumptions for surface scattering. It was in the pursuit of an explanation for the line shape of this experiment that we introduced the ineffectiveness parameter in our calculations. As discussed below (in connection with Figs. 5 and 6), we did find a possible explanation in terms of the ineffectiveness parameter.

(e) The signal reversal between the BS and BA lines is present in all RFSE lines for both surface scattering assumptions, thus making obvious the fact that the interference between the driving currents at one skin layer of the plate and the currents transmitted by the effective bulk trajectories from

the second skin layer is basic for the existence of the RFSE lines. To add to this point of view, it is evident from Fig. 2 that there is no reversal between the BA and BS surface impedance curves for $H/H_d < 1$, where this interference is absent, as expected.

(f) The approximate derivative relationship between the $R(H)$ and $X(H)$ curves, which makes the extrema of R (in the region $H/H_d > 1$) coincide with the points of maximum variation of X , is present in both specular and diffuse curves.

The variation of the RFSE line shapes with respect to the ratio of the bulk mean free path to the thickness of the plate, $\kappa = l/d$, is shown in Fig. 3 for both cases of diffuse and specular surface scattering. The following features are to be noticed:

(a) The amplitude of the resonant features of the diffuse line shapes increases with κ due to the increased effectiveness of the bulk trajectories to bring currents from the one skin layer to the other. In fact, the initial dip in R (diffuse, BA) increases more rapidly than the other parts of the line with increasing κ as a result of the more effective coupling between the bulk trajectories and the electric field at the regions of its largest amplitude, namely, just inside the surfaces.

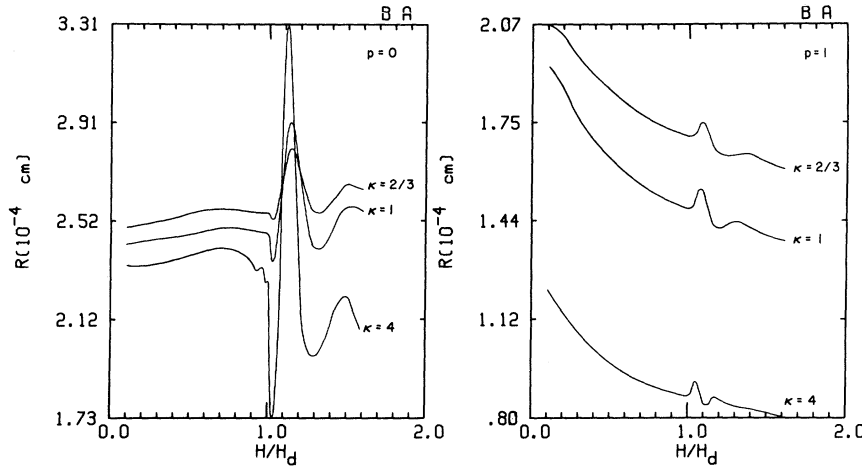


FIG. 3. Variation of $R(H)$ with κ , the ratio of the bulk mean free path to the thickness of the plate, for both values of the specularity parameter, $p=0$ and $p=1$.

On the other hand, the amplitudes of the resonant structure in the specular lines remain unaltered or even decrease slightly with increasing κ . This unexpected result is consistent with the explanation put forth in the discussion of Fig. 2 [observation (c)]. In the specular case both the effectiveness of the bulk trajectories and the effectiveness of the opposing skipping surface trajectories increase with κ . In fact, the surface trajectories seem to have the upper hand in this interference, thus accounting for the slight decrease of the amplitude of the resonant features of the specular lines with increasing κ .

(b) Decreasing κ increases the over-all average value of the surface resistance, as expected. The rate of this vertical shift of the surface impedance curves is faster in the specular than it is in the diffuse case. Thus, both the "base line" and the resonant structure of the surface impedance have a dependence on κ which is different for the two surface scattering assumptions.

(c) In both cases of surface scattering, the extrema of the RFSE lines shift to the left, i.e., toward H_d , with increasing κ . The lines also become narrower with increasing κ ; this in turn means that the effective penetration depth of the rf field decreases with increasing κ .

The differences cited above on the mean-free-path dependence of both specular and diffuse lines should allow one to decide, from a study of $Z(H)$ as a function of temperature, which of these two extreme mechanisms is more predominant (for a given experiment).

In Fig. 4, we show the surface resistance for various choices of p , the Fuchs specularity parameter mentioned in Sec. I. [$S(\theta)=p$, $0 \leq p \leq 1$, for all angles of incidence θ ; $\eta=1$; $\kappa=1$]. In this case we note the following features:

(i) As p decreases from its maximum ($p=1$) to

its minimum ($p=0$) value, the peak of $R(BA)$ at $H/H_d = 0$ seems to disappear.

(ii) The initial dip in $R(BA)$ immediately after $H/H_d = 1$ has its maximum amplitude for $p=0$, while it disappears completely for $p=1$.

(iii) The large positive peak in $R(BA)$ following the initial dip discussed in (ii) not only increases in amplitude as p decreases from one to zero but it also shifts to higher values of magnetic field.

(iv) As the surface scattering becomes more and more diffuse, the average value of $R(BA)$ or $R(BS)$ over the whole range of magnetic fields increases, as expected. The main general feature of Fig. 4 is that for values of p such that $0 < p < 1$ the profile of the surface impedance is intermediate between the diffuse and the specular profile.

The structure of $R(H)$ in the BA mode of excitation for various choices of θ_0 in the particular specular function

$$S(\theta) = 1 \text{ for } \theta \leq \theta_0, \quad S(\theta) = 0 \text{ for } \theta > \theta_0 \quad (3.1)$$

has been published in a recent letter.⁴ The main result of that calculation was the prediction that, if there is strong angular dependence in surface scattering, such as that expressed in (3.1), then one should be able to probe it experimentally through the changes in R occurring at magnetic fields smaller than H_d , the critical magnetic field of the RFSE line.

In all of the RFSE line shapes studied so far in Figs. 2-4 or in Ref. 4, the initial dip in $R(BA)$ immediately after $H/H_d = 1$ is not sharp enough to agree with the RFSE line shape observed in potassium by Walsh *et al.*¹² However, from the results already presented it is apparent that the more diffuse the surface scattering the larger the amplitude of the dip in $R(BA)$. In the context of the Fuchs specularity parameter, surface scattering cannot be made more diffuse than the situa-

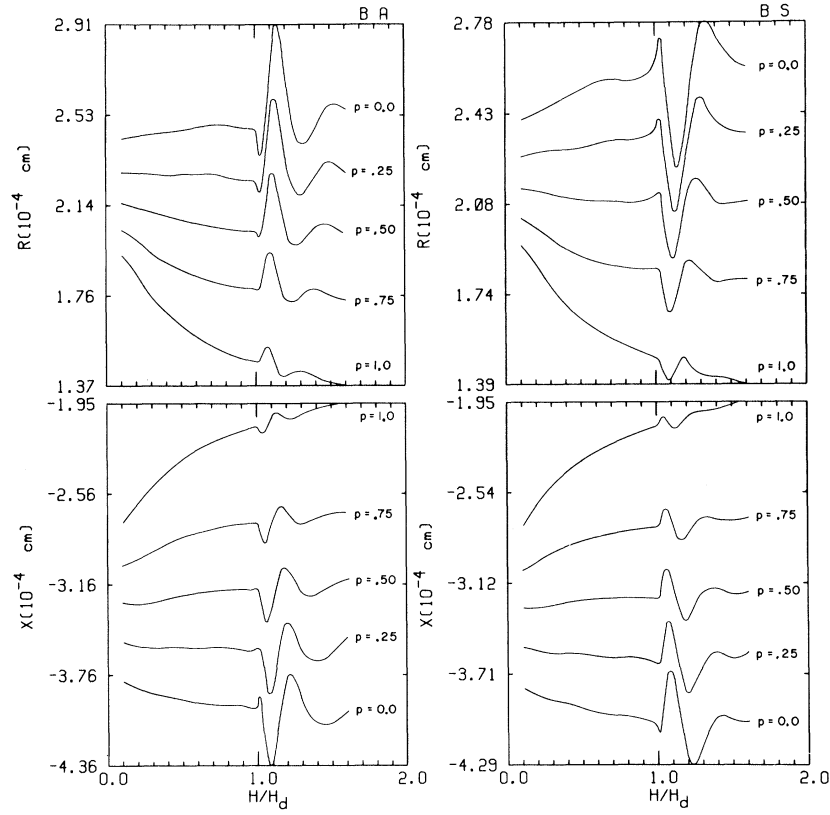


FIG. 4. Variation of $R(H)$ and $X(H)$ (for both the BA and the BS modes) with the specularity parameter p .

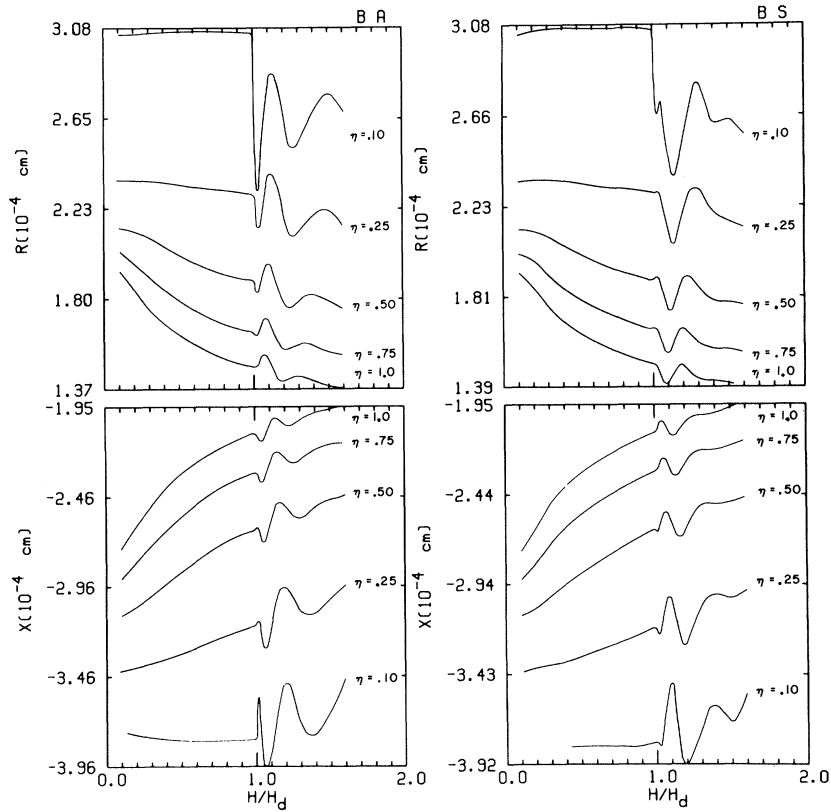


FIG. 5. Variation of $R(H)$ and $X(H)$ (for both the BA and the BS modes) with the ineffectiveness parameter η .

tion in which $p = 0$. This inability of the specularity parameter to bring forth the contrast between the surface trajectories present in the region $H/H_d < 1$ and the bulk trajectories only present in the region $H/H_d > 1$ prompted the investigation of $Z(H)$ as a function of the ineffectiveness parameter η . The results are shown in Fig. 5 [for $S(\theta) = 1$ for all θ and $\kappa = 1$]. Here again the dip in R (BA) increases with decreasing η to become almost step-like in the case $\eta = 0.10$. This sharp decrease in R at $H/H_d = 1$ (which is independent of the symmetry of the exciting currents, thus asserting that its origin is due to surface scattering rather than interference between driving and transmitted surface currents) produces the large negative spike in $\partial R/\partial H$ shown in Fig. 6(b) with the corresponding experimental line¹² for potassium shown in Fig. 6(d). The other experimental line observed also in K¹⁰ is shown in Fig. 6(c) with the corresponding calculated line shape for $\eta = 1$ shown in Fig. 6(a). The good qualitative agreement of the calculated line shapes with those experimentally observed in K leads to the conclusion that it is possible to reconcile two obviously different experimental results in terms of the ineffectiveness parameter alone, if it is true that the surface preparation in the two experiments were so different as to justify the large difference in the values of η used to calculate the two line shapes.

IV. CONCLUSION

In the absence of a microscopic theory of surface

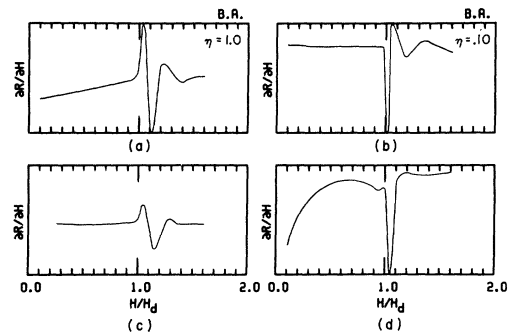


FIG. 6. Qualitative comparison with experiment. (a) $\partial R/\partial H$ as calculated in the present work with $\kappa = 1$, $\omega/2\pi = 1$ MHz and $\eta = 1$; (b) $\partial R/\partial H$ as calculated in the present work with $\kappa = 1$, $\omega/2\pi = 1$ MHz and $\eta = 0.10$; (c) experimental $\partial R/\partial H$ in potassium as reported in Ref. 10 ($\kappa \approx \frac{1}{3}$, $\omega/2\pi = 1.5$ MHz); (d) experimental $\partial R/\partial H$ in potassium as reported in Ref. 12 ($\kappa \approx 4$, $\omega/2\pi = 32.69$ MHz). The amplitudes of the calculated curves have not been scaled with respect to the amplitudes of the experimental curves.

scattering, it seems that the kinetic formulation presented in this and previous papers by the author contains enough ingredients to provide meaningful comparison with experiment in terms of phenomenological parameters, such as the specularity function and the ineffectiveness factor. From such comparisons, in turn, one might be able to give substance to these parameters by constructing the lacking microscopic theory of surface scattering.

*Research supported by the U. S. Atomic Energy Commission in part (and in part by the U. S. Office of Naval Research and the National Aeronautics and Space Administration, while the author was at the University of Chicago, Chicago, Ill.).

¹V. F. Gantmakher, in *Progress in Low-Temperature Physics*, edited by C. J. Gorter (North-Holland, Amsterdam, 1966), Vol. 5, p. 181.

²J. M. Ziman, *Principles of the Theory of Solids* (Cambridge U. P., Cambridge, England, 1964).

³K. Fuchs, Proc. Cambridge Phil. Soc. **34**, 100 (1938).

⁴G. E. Juras, Phys. Rev. Letters **24**, 390 (1970).

⁵G. A. Baraff, Phys. Rev. **187**, 851 (1970).

⁶G. E. Juras, Phys. Rev. **187**, 784 (1970).

⁷R. G. Chambers, Proc. Roy. Soc. (London) **A65**, 458 (1952).

⁸W. M. Walsh, Jr. (private communication).

⁹G. E. H. Reuter and E. H. Sondheimer, Proc. Roy. Soc. (London) **A195**, 336 (1948).

¹⁰J. F. Koch and T. K. Wagner, Phys. Rev. **151**, 467 (1966).

¹¹J. F. Koch, in *Solid State Physics*, edited by J. F. Cochran and R. R. Haering (Gordon and Breach, New York, 1968), Vol. 1, p. 253.

¹²P. S. Peercy, W. M. Walsh, Jr., L. W. Rupp, Jr., and P. H. Schmidt, Phys. Rev. **171**, 713 (1968).